PROCEEDINGS OF SCIENCE

Event shape and jet substructure measurements in high Q^2 deep inelastic scattering at HERA

Zhiqing Zhang[†,*]

[a] *ILaboratoire de Physique des 2 infinis Irène Joliot-Curie – IJCLab, Université Paris-Saclay, Bât. 100, 15 rue Georges Clémenceau, Orsay, France*

E-mail: Zhiqing.Zhang@ijclab.in2p3.fr

Measurements of event shapes and jet substructure observables can serve as in-depth probes of the strong interactions. Data on deep-inelastic scattering collected at the HERA ep collider using the H1 detector have been analysed in the kinematic region of large momentum transfer $Q^2 > 150\,\mathrm{GeV}^2$. Various new measurements of the hadronic final state, as listed in the following, are presented and are confronted with QCD calculations and predictions from Monte Carlo generators. A precision measurement of the 1-jettiness event shape is presented as a triple-differential cross section in Q^2, y, and the event shape τ_1^b. The data are sensitive to parton distribution functions, to the strong coupling α_s, and to fragmentation effects. It is also interesting to study the effect of grooming techniques on event shapes in the clean environment of ep collisions. The grooming techniques investigated here are based on the novel Centauro jet algorithm, which has the advantage to suppress soft QCD radiation in the forward (proton) direction. Two groomed event shapes are studied for various settings of the grooming parameter: the invariant jet mass and the 1-jettiness. The groomed event shape measurements show sensitivity to fragmentation on one hand and multi-jet production on the other hand. As such, they serve as high-precision probes of the tested QCD models and predictions. Another class of observables presented here is related to jet substructure. A number of jet substructure variables such as jet charge, particle multiplicity, and higher moments of these, are unfolded (corrected for detector effects) in a simultaneous and unbinned machine-learning approach. The results are shown in four regions of Q^2. Due to the unbinned nature of the unfoldings, other observables and correlations could be studied in the future. Finally, jet substructure is also investigated in terms of a charge asymmetry, defined for the leading and subleading charged particles of the jet. The charge asymmetry is studied as a function of the formation time, which gives detailed insights on the fragmentation into hadrons.

41st International Conference on High Energy physics - ICHEP2022
6-13 July, 2022
Bologna, Italy

[*] Speaker
[†] for the H1 Collaboration

PoS(ICHEP2022)769

This talk covers four preliminary results [1–4] from the H1 Collaboration at HERA. H1 was a general purpose detector at the unique electron-proton collider HERA, operated in two phases over 15 years until 2007. The neutral and charged current deep inelastic scattering (DIS) processes are the dominant processes and their measured cross sections have been the primary source for constraining the parton distribution functions (PDFs) of the proton. Preserved data and the modernised analysis code [5] have been actively used in recent years as a testing ground for a future electron ion collider (EIC). The four analyses presented here are all based on data samples taken by the H1 detector in the years 2003-2007 corresponding to an integrated luminosity of about $350\,\mathrm{pb}^{-1}$ at a centre-of-mass energy of 319 GeV. The bulk kinematic regions covered are at high Q^2 above $150\,\mathrm{GeV}^2$, with Q^2 being the negative four-momentum transfer squared, for inelasticity y values between 0.2 and 0.7.

The first result concerns a precise measurement of 1-jettiness in the Breit Frame at high Q^2. The general N-jettiness τ_N for events with N-jets and a number of initial-state beam directions of N_B was introduced in Ref. [6] (for DIS $N_B = 1$). The 1-jettiness τ_1^b is a special case when $N = 1$: $\tau_1^b = 2/Q^2 \sum_{i\in X} \min\{q_B \cdot q_i, q_J \cdot p_i\}$ where the sum runs over each particle i with momentum p_i belonging to hadronic particle state X, $q_B = xP$ and $q_J = q + xP$ with x being the Bjorken variable and P the initial proton beam momentum [7]. Differential cross sections $d\sigma/d\tau_1^b$ are measured both in the kinematic region of $150 < Q^2 < 20\,000\,\mathrm{GeV}^2$ and $0.2 < y < 0.7$ and in each of (Q^2, y) bins combining 9 Q^2 bins and 4 y bins in a slightly extended y region 0.1–0.9. The measurement in the inclusive region is presented in Figure 1 and is compared with different event generators Djangoh 1.4 [8], Rapgap 3.1 [9] and Pythia 8.303 [10] with the Dire parton shower [11], as well as with perturbative predictions obtained using the program NNLOJET [12] including non-perturbative (NP) corrections, showing the potential to optimise multi-purpose MC event generators and the sensitivity to determine the strong coupling constant α_s, probe hadronisation and resummation effects and constrain the PDFs.

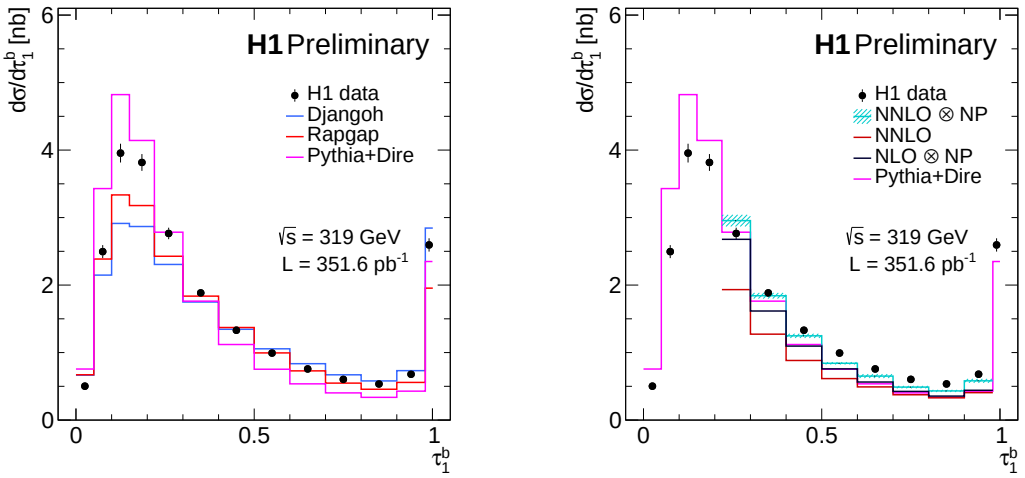

Figure 1: Measured $d\sigma/d\tau_1^b$ in the kinematic region of $150 < Q^2 < 20\,000\,\mathrm{GeV}^2$ and $0.2 < y < 0.7$ in comparison with predictions from different MC generators and fixed-order calculations.

The second measurement is on the groomed event shapes in high Q^2 DIS. Event shapes provide

incisive probes of QCD, both its perturbative and NP aspects. Grooming techniques [13] are applied for the first time to DIS events, grooming away QCD initial state radiation, beam remnant, wide-angle and soft radiation, leaving effectively only fragments of the struck parton. The procedure starts by clustering all particles in an event into a clustering tree with the Centauro jet algorithm [14]. It iteratively de-clusters the tree in the order it was clustered and compares $z_i = P \cdot p_i / P \cdot q$ (with P and p_i sharing the same definition given above and q being the four-momentum of the exchanged virtual boson in the neutral current DIS process) of the branches at each step by removing the branch with the smaller z_i if it satisfies the grooming condition with $\min(z_i, z_j)/(z_i + z_j) < z_{\text{cut}}$ and keeping the remaining branch subdivided. The procedure continues until the grooming condition is met. Groomed τ_1^b and groomed invariant mass (GIM) are measured for different values of z_{cut} varying from 0.05 to 0.2. Two examples are shown in Figure 2. The measurements are compared with predictions from MC generator Herwig 7.2 [15] and Pythia 8.3 [10]. The large values of τ_1^b are dominated by fixed-order behaviour while the low values are sensitive to single jet evolution and hadronisation. Similarly, the middle and low GIM region is sensitive to radiation pattern inside a jet (jet substructure) and hadronisation while the large GIM region is due to multijet production.

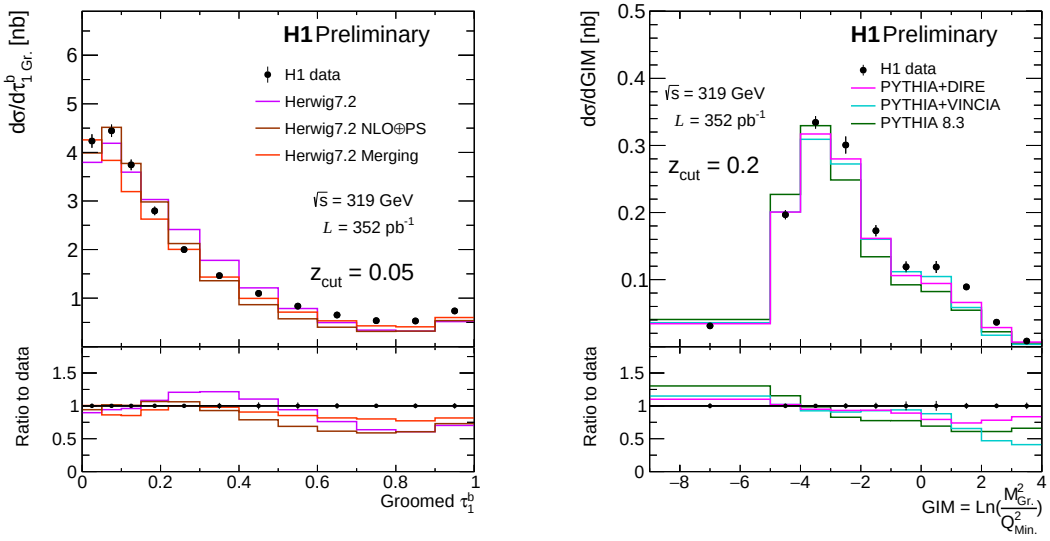

Figure 2: Measurements of groomed τ_1^b at $z_{\text{cut}} = 0.05$ (left) and groomed invariant mass (GIM) at $z_{\text{cut}} = 0.2$ (right) in the kinematic region of $150 < Q^2 < 20\,000\,\text{GeV}^2$ and $0.2 < y < 0.7$ in comparison with predictions from different MC generators.

The third measurement concerns the jet substructure at high Q^2 using machine learning. At high energy particle colliders, outgoing partons manifest as collimated sprays of particles known as jets. The jet substructure provides insight into the emergent properties of QCD at high energies. Previously the jet substructure was probed by a generalised set of jet angularities [16] $\lambda_\beta^\kappa = \sum_{i \in \text{jet}} z_i^\kappa \, (R_i/R_0)^\beta$ with z_i representing the ratio $p_{\text{T},i}/p_{\text{T}}^{\text{jet}}$ for a particle with transverse momentum $p_{\text{T},i}$ clustered inside a jet with momentum $p_{\text{T}}^{\text{jet}}$ and distance parameter R_0, and R_i describing the distance between the particle and the jet axis.

In this analysis it is extended by including the electric charge information from hadrons q_i clustered inside the jet: $\tilde{\lambda}_0^\kappa = Q_\kappa = \sum_{i \in \text{jet}} q_i \times z_i^\kappa$ to define six jet observables: jet charge $\tilde{\lambda}_0^1$,

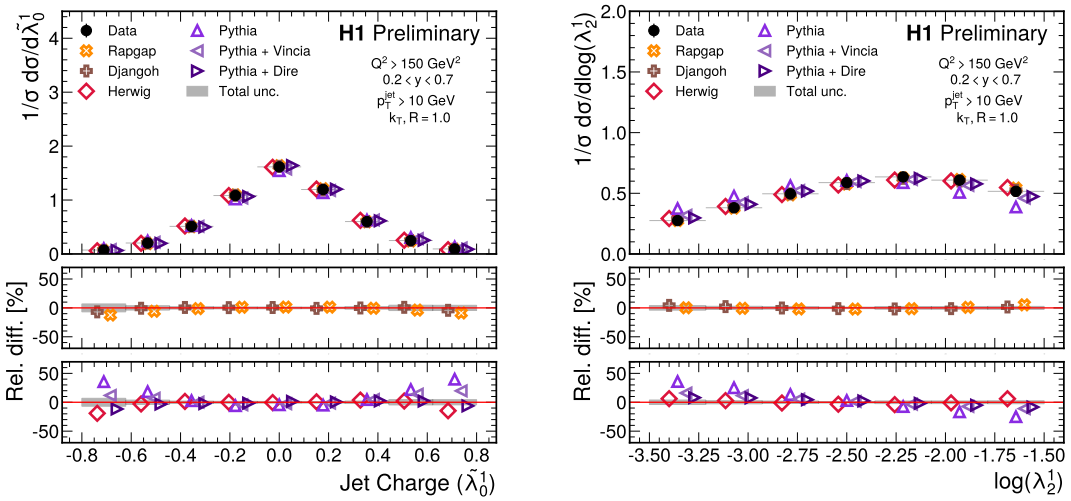

Figure 3: Measured cross sections, normalised to the inclusive jet production cross section, as a function of jet charge $\tilde{\lambda}_0^1$ (left) and jet thrust λ_2^1 (right) in the kinematic region of $150 < Q^2 < 20\,000\,\text{GeV}^2$ and $0.2 < y < 0.7$ in comparison with predictions from different MC generators.

charged hadron multiplicity $\tilde{\lambda}_0^0$, momentum dispersion $p_T D^2 = \lambda_0^2$, jet broadening λ_1^1, jet thrust λ_2^1 and an intermediate observable $\lambda_{1.5}^1$.

All the observables are then unfolded simultaneously by using reconstructed particles inside jets as inputs without binning to a graph neural network and the machine learning based method Omnifold [17]. The unfolded results for two observables for events with $Q^2 > 150\,\text{GeV}^2$ and $0.2 < y < 0.7$ are presented in Figure 3 and compared with predictions from different MC generators.

Normalised multi-differential results are also obtained probing the jet substructure evolution as a function of the energy scale Q^2 and providing complementary information to planned studies on jet substructure at the EIC.

The final result is related to the measured charged asymmetry jet substructure in DIS. A charge correlation relation is defined [18]

$$r_c(X) = \frac{\frac{d\sigma_{h_1 h_2}}{dX} - \frac{d\sigma_{h_1 \bar{h}_2}}{dX}}{\frac{d\sigma_{h_1 h_2}}{dX} + \frac{d\sigma_{h_1 \bar{h}_2}}{dX}}$$

where h_1 and h_2 represent the leading and next-to-leading charged hadron, respectively, in a jet, reconstructed with the anti-k_t algorithm with distance parameter $R_0 = 1$. Several observables X are measured in particular the formation time t_{form} giving the information on when the di-hadron fragmentation occurred. A recursive soft drop (RSD) algorithm [19] is then applied to the leading jet of the event to remove soft wide-angle emissions and probe the substructure by imposing the RSD condition $\min(p_{T,1}, p_{T,2})/(p_{T,1} + p_{T,2}) < z_{\text{cut}}(\Delta R_{12}/R_0)^\beta$ with $z_{\text{cut}} = 0.2$ and $\beta = 1$. Two categories of events are selected: one when the h_1 and h_2 are resolved in the first prong or split ($n_R = 1$) and the other when they are resolved when $n_R \geq 2$. The results as functions of t_{form} and jet transverse momentum $p_{T,\text{jet}}$ are shown in Figure 4 and again compared with predictions from

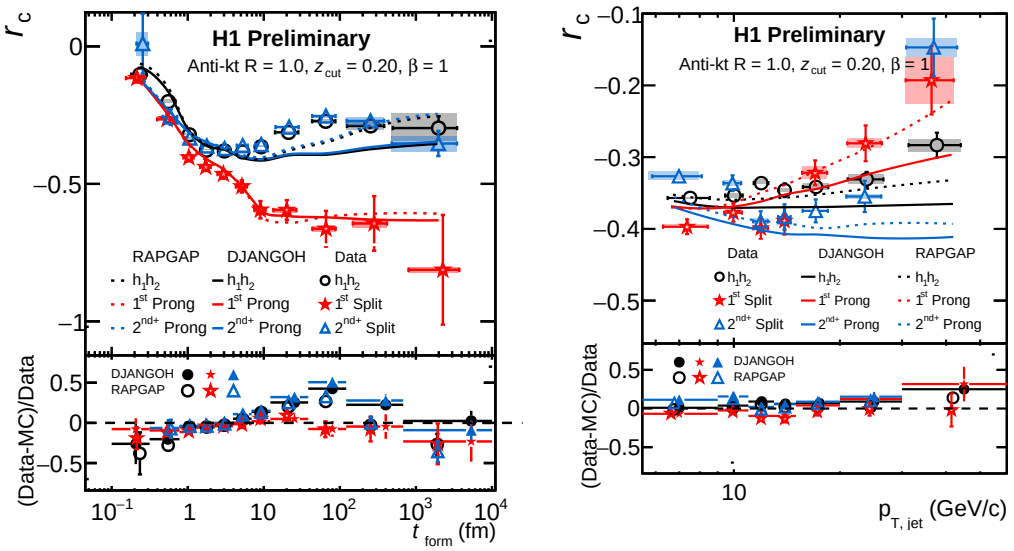

Figure 4: Measurement of r_c as a function of t_{form} (left) and $p_{\text{T, jet}}$ (right) in comparison with predictions from different MC generators.

different MC generators. The small formation time ($\sim$ 1 fm) has of small z origin and corresponds to the region, purely perturbative in nature, where leading and next-to-leading particles originate from early decorrelations, whereas the large formation time ($\gtrsim$ 10 fm) corresponds to NP in nature. It is striking that the charge asymmetry of the first split at large t_{form} is stronger than that of the subsequent splits.

To conclude, the preserved H1 data have been exploited with new ideas, person-powers, and modern analysis techniques. Four preliminary measurements have been presented. These measurements are sensitive to strong coupling constant α_s, parton distributions functions, transverse momentum distributions, hadronisation, and resummation effects. They are also useful for improving event generators, parton shower models, for better understanding of hadronisation dynamics, and for stimulating theory community to provide improved or higher order predictions.

References

[1] H1 Collaboration, Measurement of 1-jettiness in the Breit Frame at high Q^2, https://www-h1.desy.de/h1/www/publications/htmlsplit/H1prelim-21-032.long.html.

[2] H1 Collaboration, Groomed event shapes in high Q^2 DIS, https://www-h1.desy.de/h1/www/publications/htmlsplit/H1prelim-22-033.long.html.

[3] H1 Collaboration, Jet substructure at high Q^2 using machine learning, https://www-h1.desy.de/h1/www/publications/htmlsplit/H1prelim-22-034.long.html.

[4] H1 Collaboration, Charged asymmetry jet substructure in DIS, https://www-h1.desy.de/h1/www/publications/htmlsplit/H1prelim-22-032.long.html.

[5] D. Britzger, S. Levonian, S Schmitt, and D. South for the H1 Collaboration, EPJ Web Conf. **251** (2021), 03004 doi:10.1051/epjconf/202125103004 [arXiv:2106.11058 [hep-ex]].

[6] I. W. Stewart, F. J. Tackmann and W. J. Waalewijn, Phys. Rev. Lett. **105** (2010), 092002 doi:10.1103/PhysRevLett.105.092002 [arXiv:1004.2489 [hep-ph]].

[7] D. Kang, C. Lee and I. W. Stewart, Phys. Rev. D **88** (2013), 054004 doi:10.1103/PhysRevD.88.054004 [arXiv:1303.6952 [hep-ph]].

[8] K. Charchula, G. A. Schuler and H. Spiesberger, Comput. Phys. Commun. **81** (1994), 381-402 doi:10.1016/0010-4655(94)90086-8

[9] H. Jung, Comput. Phys. Commun. **86** (1995), 147-161 doi:10.1016/0010-4655(94)00150-Z

[10] T. Sjöstrand, S. Ask, J. R. Christiansen, R. Corke, N. Desai, *et al.*, Comput. Phys. Commun. **191** (2015), 159-177 doi:10.1016/j.cpc.2015.01.024 [arXiv:1410.3012 [hep-ph]].

[11] S. Höche and S. Prestel, Eur. Phys. J. C **75** (2015) no.9, 461 doi:10.1140/epjc/s10052-015-3684-2 [arXiv:1506.05057 [hep-ph]].

[12] T. Gehrmann, A. Huss, J. Mo and J. Niehues, Eur. Phys. J. C **79** (2019) no.12, 1022 doi:10.1140/epjc/s10052-019-7528-3 [arXiv:1909.02760 [hep-ph]].

[13] Y. Makris, Phys. Rev. D **103** (2021) no.5, 054005 doi:10.1103/PhysRevD.103.054005 [arXiv:2101.02708 [hep-ph]].

[14] M. Arratia, Y. Makris, D. Neill, F. Ringer and N. Sato, Phys. Rev. D **104** (2021) no.3, 034005 doi:10.1103/PhysRevD.104.034005 [arXiv:2006.10751 [hep-ph]].

[15] J. Bellm, S. Gieseke, D. Grellscheid, S. Plätzer, M. Rauch, *et al.*, Eur. Phys. J. C **76** (2016) no.4, 196 doi:10.1140/epjc/s10052-016-4018-8 [arXiv:1512.01178 [hep-ph]].

[16] A. J. Larkoski, J. Thaler and W. J. Waalewijn, JHEP **11** (2014), 129 doi:10.1007/JHEP11(2014)129 [arXiv:1408.3122 [hep-ph]].

[17] A. Andreassen, P. T. Komiske, E. M. Metodiev, B. Nachman and J. Thaler, Phys. Rev. Lett. **124** (2020) no.18, 182001 doi:10.1103/PhysRevLett.124.182001 [arXiv:1911.09107 [hep-ph]].

[18] Y. T. Chien, A. Deshpande, M. M. Mondal and G. Sterman, Phys. Rev. D **105** (2022) no.5, L051502 doi:10.1103/PhysRevD.105.L051502 [arXiv:2109.15318 [hep-ph]].

[19] F. A. Dreyer, L. Necib, G. Soyez and J. Thaler, JHEP **06** (2018), 093 doi:10.1007/JHEP06(2018)093 [arXiv:1804.03657 [hep-ph]].